

### **Response to Referee 1:**

In my assessment of the paper in its first version I stated that revision was necessary. I had four main comments: (1) I've asked to elaborate more on the novelty of the paper, and the Authors now better state that the objective is to demonstrate the applicability of an existing method. Since HESS supports applied research, I find the objective appropriate. (2) I've also asked to include uncertainty in the framework, which was not performed (I understand this would have been not trivial) but at least discussed. (3) Regarding the definition of "risk", the paper now is more clear. (4) The references still are very US biased, but I guess that's ok for an application oriented paper. I've also read the comments of the other Reviewers and I find the responses of the Authors adequate. Given that, I am supportive now for the publication of the paper.

***Response: We thank the reviewer for their constructive comments on the original manuscript and for acknowledging the revisions we made.***

### **Response to Referee 2:**

The revised manuscript does address many of my prior comments. However, two important comments were not adequately addressed and should be addressed prior to accepting this for publication. These are explained in detail below.

***Response: We thank the reviewer for their constructive comments on the original manuscript and for acknowledging the changes that we made. We have addressed both remaining comments below.***

1) In my prior comment 3, I mentioned that by lumping a very wide range of future emissions pathways into a single pool of projections, important distinctions between the variability in projections of the future atmospheric greenhouse gas concentrations and the uncertainty in the response of the earth system to that. In their response, they show a graph (Figure 1 in the response file) demonstrating little correspondence of flooding and emissions pathway. This explanation is helpful, but two things should be added to the revised manuscript: 1) This figure should be included; 2) A sentence should be added explaining that "for this flood statistic in this basin, the projected change through mid-late 21st century is not highly dependent on the emissions pathway" or something to that extent. This is important because for other locations and impact metrics this will certainly NOT be the case (especially looking at more temperature-driven impacts later in the 21st century, and into the 22nd). Readers should not interpret this as a generalized finding that is necessarily applicable elsewhere, but should be established on a case-by-case basis.

***Response: We agree that this is an important topic for discussion and have added the figure in question to the revised manuscript (Figure 7). In addition we have revised the discussion of this point as follows to make it clear that this is not a general finding.***

***"We observed no clear trend in flood risk based on the different RCPs. This indicates that, for this flood statistic in this basin, the variability between GCM model form and initial conditions likely overwhelms the influence of greenhouse gas emissions when comparing between scenarios. Although we caution that this is not a general finding, for this application, we show that the variability between projections within any RCP scenario is larger than the difference between RCP scenarios. Harding et al. [2012] also noted similar behaviour in their study of the Colorado River Basin." (Revised Manuscript, page 11 lines 4-9)***

2) Also part of my prior comment 3 I had noted that there did not appear to be a need to include all 234 projections. In my suggestion that a smaller ensemble of GCMs be selected, the authors focused on the difficulty in selecting GCMs, but missed my larger point (I can see from my wording how this could have been misinterpreted). I agree with the authors that selecting GCMs for an impact study is not well established, and many studies have shown that randomly selected ensembles of GCMs generally provide uncertainty estimates similar to those of any skill-based selection method. But some of the same references cited by the authors in their response (e.g., Pierce et al., 2009) show that after 10-14 GCMs are included in an ensemble of projections, little is gained by adding more projections. In a similar study to the submitted manuscript, Harding et al. (HESS, 2012) used all available projections (112 CMIP3 projections from the USBR website), but found that any randomly chosen set of 48 produced indistinguishable results (they did not look at smaller subsets). Thus, the use of 234 projections appears to be overkill by at least an order of magnitude. My concern here is that if others were to attempt to use this study to guide an effort, they could unnecessarily feel the need to include hundreds of projections, when using a dozen or two would almost certainly provide the same answers. What I would recommend at this point is that the authors include a sentence in the text (and perhaps in the conclusions as well) explaining this, such as “While we include 234 projections of future climate in this study, others (Pierce et al, 2009; Harding et al, 2012,...) have demonstrated that considerably smaller sets of projections can provide comparable results.”

***Response: We thank the reviewer for clarifying their point and we agree that other studies have demonstrated good results with smaller subsets of projections. We still think that there is a lower limit to the number of projections needed. For example, Harding et al. (2012) conclude that “impact analyses relying on one or a few climate scenarios are unacceptably influenced by the choice of projections”. However, we still appreciate the comment. The referee is correct in pointing out that in this study we have not quantified the minimum number of projections needed to achieve the same result and we would not want others to be intimidated away from this approach with the impression that the complete suite of GCM projections is a prerequisite for analysis. As such, we have revised the text as follows:***

***“We analysed 234 projections generated by 37 different climate models from the CMIP-5 (Coupled Model Intercomparison Project Phase 5) archive [Taylor et al., 2012]. In the absence of objective guidance in contemporary climate literature to limit the number of projections, we chose to include all of the available CMIP-5 projections of future climate in this study. However, it should be noted that other studies have demonstrated that a subset of projections could provide comparable results for specific study objective (e.g., water supply) [Pierce et al, 2009; Harding et al, 2012].” (Revised Manuscript, page 22 lines 14-22)***

1 **Climate change and non-stationary flood risk for the Upper**  
2 **Truckee River Basin**

3 **L. E. Condon<sup>1,2</sup>, S. Gangopadhyay<sup>1</sup> and T. Pruitt<sup>1</sup>**

4 [1]{Bureau of Reclamation Technical Service Center, Denver, Colorado}

5 [2]{Hydrologic Science and Engineering Program and Department of Geology and  
6 Geological Engineering, Colorado School of Mines, Golden, Colorado}

7 Correspondence to: L. E. Condon (lcondon@mymail.mines.edu)

8

9

1 **Abstract**

2 Future flood frequency for the Upper Truckee River Basin (UTRB) is assessed using non-  
3 stationary extreme value models and design life risk methodology. Historical floods are  
4 simulated at two UTRB gauge locations, Farad and Reno using the Variable Infiltration  
5 Capacity (VIC) model and non-stationary Generalized Extreme Value (GEV) models. The  
6 non-stationary GEV models are fit to the cool season (November-April) monthly maximum  
7 flows using historical monthly precipitation totals and average temperature. Future cool  
8 season flood distributions are subsequently calculated using downscaled projections of  
9 precipitation and temperature from the Coupled Model Intercomparison Project Phase-5  
10 (CMIP-5) archive. The resulting exceedance probabilities are combined to calculate the  
11 probability of a flood of a given magnitude occurring over a specific time period (referred to  
12 as flood risk) using recent developments in design life risk methodologies. This paper  
13 provides the first end-to-end analysis using non-stationary GEV methods coupled with  
14 contemporary downscaled climate projections to demonstrate the evolution of flood risk  
15 profile over typical design life periods of existing infrastructure that is vulnerable to flooding  
16 (e.g. dams, levees, bridges, and sewers). Results show that flood risk increases significantly  
17 over the analysis period (from 1950 through 2099). This highlights the potential to  
18 underestimate flood risk using traditional methodologies that don't account for time varying  
19 risk. Although model parameters, for the non-stationary method are sensitive to small changes  
20 in input parameters, analysis shows that the changes in risk over time are robust. Overall,  
21 flood risk at both locations (Farad and Reno) is projected to increase 10-20% between the  
22 historical period 1950-1999 and the future period 2000-2050 and 30-50% between the same  
23 historical period and 2050-2099.

24

## 1 1 Introduction

2 “Stationarity is Dead” [Milly et al., 2008], yet the standard practice for flood frequency  
3 analysis is predicated on this very assumption. This discrepancy has not gone unnoticed  
4 within the scientific community and there is a growing body of research investigating, (1)  
5 trends in observed floods [e.g. Franks, 2002; Vogel et al., 2011], (2) ways to incorporate non-  
6 stationarity into frequency distributions [e.g. Katz and Neveau, 2002; Raff et al., 2009~~5~~] and  
7 (3) methodologies to interpret risk and approach design within a non-stationary framework  
8 [e.g. Mailhot and Duchesne, 2010; Rootzen and Katz, 2013; Salas and Obeysekara, 2014].  
9 Both the frequency and intensity of extreme events are particularly susceptible to change  
10 because small shifts in the center of a distribution can potentially have much larger impacts  
11 on the tails [Meehl et al., 2000]. Regardless of climate change, naturally occurring long-term  
12 climate oscillations, such as ENSO, have been linked to low frequency variability in flood  
13 frequency [e.g. Cayan et al., 1999; Jain and Lall, 2001]. Anthropogenic climate change has  
14 the potential to amplify natural climatic variability throughout the interconnected climate and  
15 hydrologic systems.

16 Already trends in many hydrologic variables have been observed across the ~~w~~Western United  
17 ~~S~~States (as well as around the world). For example, clear increases in temperature have been  
18 measured across the west [e.g. Cayan et al., 2001; Dettinger and Cayan, 1995]. Precipitation  
19 trends are more variable. Regonda et al. [2005] found increased total winter precipitation (rain  
20 and snow) from 1950 to 1999 in many sites across the western United States, although  
21 springtime snow water equivalent (SWE) was shown to decline over the same period.  
22 Similarly, Mote et al. [2005] ~~analyzed~~analysed snowpack trends in western North America,  
23 and reported widespread declines in springtime SWE over the period 1925–2000, especially  
24 since the middle of the 20th century. They attribute this decline predominantly to climatic  
25 factors such as El Niño–Southern Oscillation (ENSO), Pacific Decadal Oscillation (PDO),  
26 and positive trends in regional temperature. Easterling et al. [2000] summarized previous  
27 studies on precipitation trends. They note that trends vary from region to region, but in  
28 general, increases in precipitation have occurred disproportionately in the extremes. Several  
29 subsequent studies have observed increasing trends in extreme precipitation events, although  
30 the changes are relatively small [Gutowski et al., 2008; Kunkel, 2003; Madsen and Figdor,  
31 2007].

1 Research has also demonstrated increasing trends in flood frequency in some regions. Walter  
2 and Vogel [2010] and Vogel et al. [2011] observed increasing flood magnitudes across the  
3 United States using stream gauge records, and Franks [2002] showed statistically significant  
4 increases in flood frequency since the 1940s. Still, non-stationary flood behaviour has been  
5 historically difficult to quantify and there has been some debate on the significance of flood  
6 frequency trends. For example, Hirsch [2011] noted both increasing and decreasing trends in  
7 annual flood magnitudes in different regions of the US. Also, Douglas et al. [2000] found that  
8 if one takes into account spatial correlation, many previous findings of flood trends are not  
9 statistically significant. Difficulty in diagnosing flood trends is not unique to the ~~w~~Western  
10 US; a literature review of historical flood studies across Europe also found spatial variability  
11 in flood trends [Hall et al., 2014].

12 Even when significant trends are found, the complexity of flooding mechanisms that depend  
13 on many variables ~~which~~and can vary regionally and seasonally, makes it difficult to attribute  
14 trends to specific causes. Illustrating the importance of seasonality, Small et al. [2006]  
15 showed that if a high precipitation event occurs in the fall, as opposed to the spring, it will  
16 contribute to baseflow rather than inducing flooding. Also, urbanization can drastically  
17 increase the impervious area of a basin, thus amplifying floods by decreasing infiltration and  
18 speeding runoff. The largest flood magnitude increases observed by both Walter and Vogel  
19 [2010] and Vogel et al. [2011] were in basins with urban development. The influence of  
20 development trends on flood ~~behavior~~behaviour can be difficult to separate from other  
21 variables. For example, Villarini et al. [2009] could not conclusively tie reduced stationarity  
22 (i.e. changes in mean and/or variance) in peak discharge records to climate change because of  
23 variability in the other factors that influence runoff.

24 Merz et al. [2012] note that attributing changes in flood hazard is complicated by the complex  
25 array of drivers that can include; land cover change and infrastructure development as well as  
26 natural climate variability and change. Here we set aside the impacts of development and  
27 management practices and focus on the role of climate change. However, even with this  
28 simplification, future extremes can still be influenced by a number of interrelated variables  
29 such as changes in temperature, precipitation efficiency, and vertical wind velocity [Mullet et  
30 al., 2011; O'Gorman and Schneider, 2009]. ~~Analyzing~~Analysing global circulation model  
31 (GCM) outputs Pierce et al. [2012] found total changes in precipitation to be small relative to  
32 the existing variability but noted larger seasonal changes in storm intensity and frequency.

1 Despite uncertainty, many studies agree that warming will increase the potential for intense  
2 rainfall [Allan, 2011; Gutowski et al., 2008; Pall et al., 2011; Sun et al., 2007]. Furthermore,  
3 Min et al. [2011] found that some GCM simulations may underestimate extreme precipitation  
4 events in the northern hemisphere. Indicating that projections of extreme precipitation based  
5 on GCM outputs may be conservative.

6 Studies have also predicted increases in flood frequency and magnitude with a warmer  
7 climate especially in snowmelt dominated basins [e.g. Das et al., 2011]. As with historical  
8 flooding trends, translating forecasted climate variables to flood frequency is a complex  
9 process and several methodologies have been used. Downscaled GCM climate forcings can  
10 be used to drive hydrologic models and simulate future floods directly [e.g. Das et al., 2011;  
11 Vogel et al., 2011; Raff et al., 2009]. With this approach, traditional stationary flood  
12 frequency distributions can be fit to the simulated floods to calculate return periods of  
13 interest [e.g. Raff et al., 2009; Vogel et al., 2011]. This allows for return periods and flood  
14 magnitudes that change over time, as with the flood magnification and recurrence reduction  
15 factors calculated by Walter and Vogel [2010] and Vogel et al. [2011]. ~~However~~ While, these  
16 approaches do capture temporal changes between analysis periods, they still assume that flood  
17 mechanisms are stationary ~~over the time period that the distribution is fitted to~~ within each  
18 period of analysis.

19 This limitation can be overcome using non-stationary generalized extreme value (GEV)  
20 distributions where the model parameters like mean (i.e. location) and spread (i.e. scale) are  
21 allowed to vary as a function of time [e.g. Gilroy and McCuen, 2012] or with relevant  
22 covariates [e.g. Griffis and Stedinger, 2007; Katz et al., 2002; Towler et al., 2010]. This  
23 approach has been gaining popularity for flood frequency estimation. Using this technique it  
24 is not necessary to simulate future floods directly by forcing a hydrologic model with  
25 projected hydroclimate fields (e.g. precipitation and temperature). The parameters of the GEV  
26 model, like mean and spread change with time (i.e. non-stationary) based on a linear  
27 combination of covariates like precipitation and temperature. Historical relationships between  
28 extreme events and hydroclimate fields are used to identify the weighting of covariates. These  
29 weights are then used to estimate parameters for future time periods using precipitation and  
30 temperature outputs from hydroclimate projections. For example, Gilroy and McCuen [2012]  
31 used non-stationary GEV models of flood frequency that incorporated a linear trend in the

1 location parameter. Similarly, Griffis and Stedinger [2007] and Towler et al. [2010] used  
2 climate variables as covariates for the distribution parameters.

3 While, non-stationary flood forecasting methods provide flexibility to analyze flood  
4 variability, they are also incongruent with many of the traditional metrics used in water  
5 resources planning. Historically, most ~~infrastructure~~infrastructures that ~~are~~is vulnerable to  
6 flooding (e.g. dams, levees, sewers and bridges) ~~have~~es been designed to withstand flooding of  
7 specified return period (e.g. the 100--year flood). However, these calculations rely on a flood  
8 frequency distribution which is assumed to remain stationary with time, and hence the return  
9 period design metric is also assumed to be stationary. When non-stationary methods are used,  
10 the underlying flood frequency distributions, and associated return periods, vary with time.  
11 Thus, under a non-stationary climate, the notion of static return period flood event (e.g., 100-  
12 year flood, 200-year flood, etc.) is no longer a valid concept.

13 To address this issue, Rootzén and Katz [2013] introduced the concept of design life level to  
14 calculate the risk of a given flood magnitude occurring over a specified time period. Salas and  
15 Obeysekera [2014] further demonstrated the relevance of this technique to the hydrologic  
16 community using flood frequency examples. However, this methodology has yet to receive  
17 widespread attention within the hydrologic community. Here, we present a non-stationary  
18 flood frequency assessment for the Upper Truckee River Basin (UTRB) using contemporary  
19 downscaled climate projections and the non-stationary design life level technique introduced  
20 by Rootzén and Katz [2013] to quantify flood risk. ~~(Note that, following the convention of~~  
21 ~~Rootzén and Katz [2013] we use the term flood risk to refer to the probability of an extreme~~  
22 ~~event occurring and not as a quantification of expected losses).~~ While the methodology used  
23 for this analysis is previously established, this paper provides the first end-to-end  
24 demonstration of non-stationary GEV analysis coupled with contemporary downscaled  
25 climate projections (specifically, downscaled climate projections from the Coupled Model  
26 Intercomparison Project Phase-5 (CMIP-5)), to quantify how the flood risk profiles may  
27 evolve in the Upper Truckee River basin ~~Basin~~ over the ~~next 21<sup>st</sup>~~ century. The flood  
28 analysis presented here is part of a larger study on climate change impacts in the Truckee  
29 River basin [~~Reclamation, 2010~~]. This project is supported by local water managers and  
30 conducted by the Bureau of Reclamation through the Water-~~Smart~~SMART Basin Studies  
31 Program authorized under U.S. Public Law 111-11, Subtitle F (SECURE Water Act). The  
32 intent of this work is <sup>(1)</sup> to investigate potential flood risk changes over time in the Truckee

Formatted: Superscript



1 | [basinUTRB](#) and (2) to demonstrate the applicability of non-stationary techniques in a regional  
2 | flood analysis to make these tools more accessible to the hydrologic community.

3 | The paper is organized as follows. Section 2 provides background on the study area along  
4 | with data sets and models used. The methodologies of using non-stationary spatial GEV  
5 | analysis in conjunction with climate projections and time evolving risk assessment are  
6 | described in section 3. Results and discussions of findings are given in section 4. Summary  
7 | and conclusions from the analysis are presented in section 5.

## 9 | **2 Background**

10 | This section provides background on the study area (2.1), streamflow data and simulations  
11 | (2.2) and climate data and models (2.3).

### 12 | **2.1 Upper Truckee River Basin**

13 | The Truckee River originates in northern Sierra Nevada Mountains in California (above Lake  
14 | Tahoe) and flows northeast to Nevada where it ends in the Pyramid Lake (Figure 1). The  
15 | total basin area is roughly 7,900 square kilometres, however the area upstream of Reno  
16 | (2,763 square kilometres) provides the majority of the basin's precipitation through  
17 | snowpack. The focus of this analysis is on the Farad and Reno gauge locations shown in  
18 | Figure 1, henceforth referred to as Farad and Reno. The Farad gauge is located roughly 1.5  
19 | [kilometerskilometres](#) downstream of the Farad hydropower plant and provides a cumulative  
20 | measure of all of the upper basin tributaries [Stokes, 2002]. Most of the available water  
21 | supply is generated upstream of the Farad ~~g~~Gauge [USACE, 2013a]. The Reno gauge is  
22 | located downstream of Farad in the heart of Reno and is a good reference point for  
23 | [analyzinganalysing](#) urban flooding. The intervening area between the Farad and Reno gauges  
24 | is small, roughly 350 square ~~kilometerskilometers~~ [km] and there are only two small  
25 | tributaries that enter the main stem between Farad ~~and Reno. (Reno Dog Creek and Hunter~~  
26 | ~~Creek).~~

27 | ———Flooding in the upper Truckee generally takes one of three forms. Some of the most  
28 | severe floods have resulted from heavy rain events covering most of the basin and lasting one  
29 | to six days. These storms generally occur from November to April and may be linked to  
30 | Atmospheric Rivers [Ralph and Dettinger, 2012]. Snowmelt floods are also common from

1 April to July. Although, snowmelt floods transmit large volumes of water for longer  
2 durations, they generally don't cause damage because they are typically well predicted and  
3 can be regulated with upstream reservoirs. Finally, in late summer (July – August), local  
4 cloudbursts can generate high intensity precipitation over small areas. These storms can  
5 cause local damage to tributaries but generally don't have a large impact on the main stem of  
6 the Truckee.

7 In the twentieth century, nine major floods have been recorded on the Truckee River,  
8 all of which occurred from November to April [USACE, 2013b]. The flood of record  
9 occurred in January of 1997 and was caused by warm rain falling on a large snowpack  
10 (~180% of normal) and melting nearly all of the snowpack below 7,000 feet [USACE,  
11 2013b]. The floods of 1950, 1955 and 1963 were some of the most damaging due to the  
12 development of Reno along the river during this time period [USACE, 2013b]. Subsequent  
13 flood damages have been, at least partially, mitigated by the implementation of flood  
14 infrastructure starting in the 1960s.

## 15 **2.2. Streamflow data and simulations**

16 — Streamflow has been measured at both the Farad and Reno USGS gauges. However,  
17 gauge flows are not readily applicable to flood frequency analysis due to upstream the  
18 presence and developments of water supply and flood control structures upstream. For  
19 example, upstream of Reno there are four dams with flood control capabilities (i.e. Martis  
20 Creek Dam, Prosser Creek Dam, Stampede Dam and Boca Dam) in addition to Tahoe,  
21 Donner and Independence Lakes which provide incidental flood regulation. Unregulated flow  
22 estimates were developed by the US Army Corps of Engineers (USACE) but are only  
23 available for historical flood eventsperiods [USACE, 2013b]. Therefore, we simulate  
24 unregulated flows from 1950 to 1999 using the three layer Variable Infiltration Capacity  
25 (VIC) model and validate results using the available unregulated flow estimates.

26 A brief summary of the VIC model is provided here, and for additional technical  
27 specifications the reader is referred to Liang et al. [1994], Liang et al. [1996] and Nijssen et  
28 al. [1997]. VIC is a gridded hydrologic model designed to simulate macro scale (spatial  
29 resolution in greater than 1 km) water balances using parameterized sub-grid infiltration  
30 and vegetation processes. In the VIC model, surface water infiltrates to the subsurface based  
31 on conductivity soil properties, and soil moisture is distributed vertically through three model

1 layers extending up to about 2 meters below the land surface. At the surface, potential  
2 evapotranspiration (PET) is simulated using the Penman Monteith PET model [Maidment et  
3 al., 1993]. Surface flows are determined in a two-step process. First, the water balance for  
4 each grid cell is calculated independently to determine surface runoff and baseflow, and  
5 subsequently runoff from each cell is routed to river channels and outlets using a predefined  
6 routing network. Here we drive VIC with daily weather forcings including precipitation,  
7 maximum and minimum temperature, and wind speed. Additional climate variables such as  
8 short and long wave radiation, relative humidity and ~~vapor~~vapour pressure are calculated  
9 within the model using established empirical relationships. The VIC model is well  
10 documented and has already been used in a number of hydrologic and climate change studies  
11 [e.g. Christensen and Lettenmaier, 2007; Christensen et al., 2004; Gangopadhyay et al., 2011;  
12 Maurer et al., 2007; Payne et al., 2004; Reclamation, 2011; Van Rheeën et al., 2004].  
13 Recently VIC has also been applied for real time flood estimation [Wu et al., [in-press2014](#)].

14 The VIC model used for this analysis was ~~developed and calibrated as~~ part of the Bureau of  
15 Reclamation's (Reclamation) West Wide Climate Risk Assessment (WWCRA) effort and is  
16 described in Reclamation [2011]. The WWCRA VIC model encompasses the western US.  
17 Simulated and observed streamflows were ~~calculated~~ ~~evaluated~~ ~~compared~~ –at 152 locations  
18 primarily from the USGS Hydroclimatic Data Network [Slack et al., 1993] and 43 additional  
19 locations of importance to Reclamation's water management activities. Among the evaluated  
20 locations are several in the Truckee basin including the Truckee River at Farad. For details on  
21 model calibration and development we refer the reader to Reclamation [2011] and  
22 Gangopadhyay et al. [2011]. While we do not discuss model calibration further here, in the  
23 subsequent sections we provide additional model verification for flood simulation in the  
24 UTRB.

## 25 **2.3 Climate data and models**

26 As noted in the previous section, the VIC model requires daily climate inputs to drive water  
27 balance simulations. We use the national 1/8° (roughly ~~12 km~~ ~~7 miles~~) gridded dataset from  
28 Maurer et al. [2002] for historical (i.e. 1950-1999) climate observations. Additionally,  
29 monthly total precipitation and average temperature were aggregated for the upstream area of  
30 each gauge for every month of the flood season (i.e. November through April). These values  
31 are used as covariates for fitting non-stationary GEV models ~~as~~ discussed in Section 3.

1 Future gridded precipitation and temperature values from 2000 to 2099 were generated from  
2 Global Circulation Model (GCM) outputs. We ~~analyzed~~analysed 234 projections generated  
3 by 37 different climate models from the CMIP-5 (Coupled Model Intercomparison Project  
4 Phase 5) archive [Taylor et al., 2012]. ~~Lacking~~In the absence of objective guidance in  
5 contemporary climate literature motivation to limit the number of projections, we chose to  
6 include all of the available CMIP-5 projections of future climate in this study. However, it  
7 should be noted that other studies have demonstrated that a subset of projections could  
8 provide comparable results for specific study objective (e.g., water supply) [Pierce et al, 2009;  
9 Harding et al, 2012]. Projections span four Representative Concentration Pathways (RCPs)  
10 for greenhouse gas emissions. Each GCM projection includes monthly gridded precipitation  
11 and temperature from 1950 to 2099 at a coarse grid resolution ranging between ~65-250  
12 ~~km~~kilometers.

13 Reclamation in collaboration with other federal and non-federal partners has developed a  
14 monthly archive of downscaled CMIP-5 projections at the finer ~~1/8°~~1/8th degree resolution  
15 using the two-step BCSD (Bias Correction and Spatial Disaggregation) algorithm described in  
16 Wood et al. [2004]. For this analysis we extended the existing hydrology archive to cover the  
17 UTRB domain for all 234 BCSD CMIP-5 climate projections following the steps detailed  
18 below. A subset of the CMIP-5 hydrology projections is publically accessible through the  
19 "Downscaled CMIP3 and CMIP5 Climate and Hydrology Projections" archive at [http://gdo-](http://gdo-dcp.ucllnl.org/downscaled_cmip_projections/)  
20 [dcp.ucllnl.org/downscaled\\_cmip\\_projections/](http://gdo-dcp.ucllnl.org/downscaled_cmip_projections/). Additional documentation on the archive and  
21 the methodology is provided in Reclamation [2014].

22 The downscaled climate variables include monthly total precipitation, monthly maximum and  
23 minimum temperatures and monthly average temperature. Before applying the BCSD  
24 algorithm all the 234 climate projections were first gridded from their respective native GCM  
25 scale to a common grid of 1° latitude by 1° longitude. Similarly, the observed 1/8° degree  
26 gridded dataset [Maurer et al., 2002] was aggregated to the coarser 1° latitude by 1° longitude  
27 grid. Next, for a given climate variable, GCM, and location (1° latitude by 1° longitude grid  
28 cell), the bias correction (BC) step uses quantile mapping between monthly CDFs  
29 (Cumulative Distribution Functions) of historical simulated and historical observed values to  
30 identify biases over a common climatological period – in this case, 1950-1999. The projected  
31 future climate variables from the same GCM at the same location are then bias corrected  
32 using the identified bias. The result of bias-correction is an adjusted GCM dataset (20th

1 century and 21st century, linked together) that is statistically consistent with the observed data  
2 during the bias-correction overlap period (i.e., 1950-1999 in this application). Note that, the  
3 BC step happens at the coarse 1° latitude by 1° longitude grid. Next, [multiplicative](#)  
4 adjustment factors ~~that are multiplicative~~ (ratio of bias-corrected GCM to observed) for  
5 precipitation and ~~an~~ offset [adjustment factors](#) (bias-corrected GCM minus observed) for  
6 temperature are calculated for each of the 1° latitude by 1° longitude grid cell [Reclamation,  
7 2013]. These adjustments are then spatially disaggregated (SD) to a 1/8° latitude by 1/8°  
8 longitude grid. Finally, the adjustments are applied (multiplicative for precipitation; additive  
9 for temperature) to the finer resolution, 1/8° degree gridded observed precipitation and  
10 temperature fields [Maurer et al., 2002] to derive the 1/8° degree gridded BCSD climate  
11 projections.

### 12 **3 Methodology**

13 This section describes the methodology used for flood frequency analysis in the UTRB.  
14 Discussion is divided into two sections. First, we describe the process of extreme value  
15 modeling using non-stationary GEV distributions (Section 3.1). Second, the methodology for  
16 design life level risk assessment is ~~described~~[detailed](#) (Section 3.2)

#### 17 **3.1 Extreme value modelling**

18 Extreme values analysis (EVA) deals with the examination of the tail (i.e. extreme) values of  
19 a distribution (as opposed to standard approaches which are generally more concerned with  
20 the average system behaviour). EVA methods are standard practice for flood frequency  
21 analysis because they are designed to capture the behaviour of low frequency high impact  
22 events. Furthermore, in climate change studies Katz [2010] points out that traditional  
23 approaches are not sufficient and extreme value statistics are needed. For this analysis, we use  
24 the Generalized Extreme Value (GEV), which is commonly applied to flood frequency  
25 analysis to model block maxima from streamflow time series [e.g. Katz et al., 2002; Towler et  
26 al., 2010]. The cumulative distribution function (CDF) for the GEV,  $F$  is as follows:

$$F(z; \theta) = \exp \left\{ - \left[ 1 + \xi \left( \frac{z - \mu}{\sigma} \right) \right]^{-1/\xi} \right\}$$

27

28

$$F(z, \theta) = \exp \left\{ - \left[ 1 + \xi \left( \frac{z - \mu}{\sigma} \right)^{\frac{1}{\xi}} \right] \right\} \quad (1)$$

Where  $z$  is the streamflow maxima value of interest and  $\theta$  is the parameter set ( $\mu$ ,  $\sigma$ ,  $\xi$ ) used to specify the distribution such that the center is given by the location ( $\mu$ ), the spread by the scale ( $\sigma$ ) and the behavior of the upper tail by the shape ( $\xi$ ). Based on the shape parameter, the GEV can take one of three forms: Gumbel, or light tailed, when  $\xi$  is zero; Fréchet, or heavy tailed, if  $\xi$  is positive; and Weibull, or bounded, when  $\xi$  is negative. Following the methodology of Towler et al. [2010], GEV parameters ( $\mu$ ,  $\sigma$ ,  $\xi$ ) are fitted using the Maximum Likelihood Estimation (MLE) technique.

In traditional stationary flood frequency analysis, it is assumed that observations are independent and identically distributed (IID), and therefore model parameters ( $\mu$ ,  $\sigma$ ,  $\xi$ ) are derived from the observed flood record and are assumed to remain constant across the period of record and into the future. Here, we introduce non-stationarity into the distribution by allowing location and scale parameters to change with relevant covariates. Such that:

$$\mu(t) = \beta_{0,\mu} + \beta_{1,\mu}x_1 + \dots + \beta_{n,\mu}x_n \quad (2)$$

$$\sigma(t) = \beta_{0,\sigma} + \beta_{1,\sigma}x_1 + \dots + \beta_{n,\sigma}x_n \quad (3)$$

Where the  $\beta$  variables represent the coefficients, and the  $x$  variables are the covariates. In keeping with previous studies the shape parameter, which is the most difficult to estimate, is assumed constant [e.g. Obeysekera and Salas, 2014; Salas and Obeysekera, 2013; Towler et al., 2010].

-Some previous studies [e.g. Salas and Obeysekera, 2013; Stedinger and Griffis, 2011] have developed non-stationary location and scale parameters that are explicitly dependent on time. This approach requires first, the derivation of temporal flooding trends and second, the projection of this trend into the future. Here we derive location and scale parameters based on time varying meteorological variables (i.e. temperature and precipitation). With the approach used here, temporal trends in flooding are introduced as a function of temporal variability in precipitation and temperature but no explicit trend is specified a priori.

Formatted: Font: Italic

Formatted: Font: Italic

1 To determine the optimal set of covariates for a non-stationary model, additional statistical  
2 methods must be employed. The Akaike Information Criterion [AIC;- Akaike, 1974], given in  
3 Equation 4, weighs the goodness of fit for a model with the level of complexity.

$$AIC = 2(\text{llh}) + 2K$$

$$AIC = 2(nllh) + 2K \quad (4)$$

6 Here *nllh* is the negative log likelihood (NLLH) estimated for a model fitted with *K*  
7 parameters. In this formulation, higher ranked models have lower AIC scores. For this  
8 analysis, the best model is selected using pairwise comparisons of NLLH scores following the  
9 methods of Salas and Obeysekera [2014] and others. Models are compared using the deviance  
10 statistic (D) which is equal to twice the difference in NLLH scores. Deviance statistics are  
11 then tested for significance based on a chi-squared distribution with the degrees of freedom  
12 set equal to the difference in the number of parameters (*K*) between models. Finally, pP-  
13 values less than 0.05 indicate a statistically significant (*alpha of 0.05*) improvement in model  
14 performance *at the 5-percent significance level*.

15 Following the methodology described above, GEV distributions are fitted to time series of  
16 maximum monthly historical (1950-1999) one day simulated stream flows (detailed in  
17 Section 2) for the cool season (*November to April*). Although, there are some unregulated  
18 historical flow estimates, the available dataset only covers six storms. Therefore, to be  
19 consistent we fit our model only to the simulated flows. The dataset includes maximum daily  
20 streamflows for each month in the cool season defined by the block of months November  
21 through April, as opposed to the more traditional single value per year. This technique was  
22 also used by Towler et al. [2010] who noted that expanding the dataset helps avoid the  
23 problems associated with using maximum likelihood estimate on small datasets. However, as  
24 noted by Towler et al. [2010], when multiple values are used per year the calculated  
25 probabilities must be adjusted appropriately to derive annual values. Floods during the cool  
26 season generally last between one and four days. Here we focus on the one day flood peak, as  
27 opposed to multi-day flood volumes, because this is a representative metric for flood damage.  
28 Additionally, using the one day flood maximum focuses the analysis on flood magnitude  
29 rather than duration.

Formatted: Font: Italic

Formatted: Font: Italic

Formatted: Font: Italic

1 -Two covariates were considered, monthly total precipitation (P) and mean temperature (T)  
2 averaged over the upstream area for each gauge. As discussed in Section 2, precipitation is a  
3 relevant covariate because many of the floods in this season are rain on snow events or  
4 extreme rainfall events. Similarly, temperature drives snowmelt and is an important  
5 contributor to UTRB flood events (e.g., January 1997 event). Both stationary and non-  
6 stationary GEV models were evaluated using the extRemes package [Gilleland and Katz,  
7 2011] in the ‘R’ statistical computing environment [JR Core Team, 2012].

### 8 3.2 Time varying risk assessment

9 Traditional flood planning relies on the concept of return periods, which are usually  
10 calculated as the inverse of annual exceedance probability for a given flood magnitude,  
11 assuming a stationary distribution. For example, the log-Pearson Type III (LP3) distribution  
12 described by the Interagency Advisory Committee on Water Data Bulletin 17B [IACWD,  
13 1982]. However, when non-stationary models are used, the distribution parameters, and  
14 hence the exceedance probabilities vary with time. Table 1 compares various flood  
15 probability calculations between stationary and non-stationary approaches [Salas and  
16 Obeysekera, 2014]. As shown here, when the flood distribution is stationary, the return  
17 period for a given flood magnitude is constant and relies only on the exceedance probability  
18 (Equation 4a in Table 1). However, if distribution parameters are non-stationary then the  
19 return period will vary based on the period of interest (Equation 4b in Table 1). This concept  
20 is easily extended to flood risk (here defined as the probability of a flood of a given  
21 magnitude occurring, not expected losses). In traditional analyses, the risk of a flood occurring  
22 in a given period depends only on the length of the period (5a), while in a non-stationary  
23 analysis risk depends on both the length of time considered and the time period itself (5b).  
24 This is the concept of design life level proposed by Rootzén and Katz [2013]. Here, we adopt  
25 the design life level risk framework given by Equation 5b in Table 1 and calculate the risk of  
26 flood for a range of future periods and design life lengths.

## 28 4 Results and Discussion

29 Results are grouped into three sections. First we present the development of the non-  
30 stationary GEV models (4.1). Next the models are verified by comparing simulated results to  
31 observations (4.2). Finally we present future projections of flood frequency analysis (4.3).



#### 4.1 Extreme value model development

A suite of models were fit to the logarithms of block (cool season, November-April) maxima flows (simulated by the calibrated VIC model) with different non-stationary parameter combinations. The model structures tested include stationary, non-stationary location, non-stationary scale and non-stationary location and scale. For all model structures, model fit was tested using one or both covariates (i.e. precipitation ~~(in)~~ and temperature ~~(F)~~). Models were also tested using the block maxima flows directly; however, performance was improved considerably with the logarithmic transformation. Validation of the VIC simulated flows as well as the GEV models are presented in the following section.

Table 2 summarizes negative log-likelihood (NLLH) and Akaike Information Criterion (AIC) scores for each model configuration. The deviance statistic (D) ~~for pairwise comparisons of~~ NLLH scores and the p-values calculated for each D based on a chi-squared distribution are also provided. ~~where~~ ~~(Note that~~ ~~T~~ the bottom row ~~of the Table 2s~~ provides the number of parameters in each model and the model number that was used for the pairwise comparisons). As shown here, the models with non-stationary location and scale relying on both precipitation and temperature as covariates have the best (i.e. lowest) NLLH scores for both stations, and are a statistically significant improvement over the other models listed in Table 2. Figure 2 plots stationary and non-stationary location and scale models with histograms of observed flow for both gauges. Qualitatively, the stationary model fits well with the center of the distribution but overestimates the tails. The non-stationary models overestimate the median values but are a closer fit to the extreme values.

The coefficients for Equations 2 and 3 for the selected models are provided in Table 3. Using the coefficients determined above, the location and scale parameters are calculated for every climate projection (i.e. 234) and flood season month (i.e. November to April 1950 to 2099) based on the downscaled precipitation and temperature values detailed in Section 2 (~~n~~Note that, the ~~shape~~ ~~scale~~ parameter remains fixed). Thus, for every future month, there is a separate GEV distribution curve for each of the 234 climate projections.

To address uncertainty of model parameters (namely, the model coefficients  $\beta$  in Equations 2 and 3), models of the same form (i.e. non-stationary location and scale with precipitation and temperature as covariates) were also fit to the historical simulation period (1950-1999) using downscaled precipitation and temperature from all 234 climate projections. Because each climate projection seeks to reproduce similar ~~historical~~ behaviour over the historical 1950-

1 | 1999 period, the variability between projections in this time frame is a measure of uncertainty  
2 | in model coefficients given the ~~same representation of the same~~ physical system. This differs  
3 | from the variability between climate projections in future periods (i.e. after 1999) which is a  
4 | measure of uncertainty in future forcing conditions. Table 3 shows the interquartile range of  
5 | model coefficients calculated from the 234 historical GCM simulations.

6 | Using these parameters the return period of the design flood at Reno (37,600cfs, 1.065cms)  
7 | was calculated for every set of model parameters using observed historical precipitation and  
8 | temperature. The observed model estimates a return period of 45 years while the interquartile  
9 | range (IQR) using the simulated model parameters (i.e., the model parameters estimated from  
10 | each of the 234 historical GCMs) with observed precipitation and temperature varies from 28  
11 | to 247 years. Note that the return period of 45-years estimated from observed meteorology is  
12 | within the IQR of 28 to 247 years. Although the IQR is large it should be kept in mind that  
13 | some of the uncertainty in this range is a result of the performance of individual GCMs in  
14 | simulating historical climate and in the BCSD downscaling methodology. The monthly  
15 | BCSD algorithm used for downscaling GCM climate only constrains the monthly  
16 | precipitation and temperature statistics (total precipitation and mean monthly temperature)  
17 | over the historical 1950-1999 period. Furthermore, uncertainty is introduced when monthly  
18 | total precipitation and mean temperature are disaggregated translated to daily values. Thus,  
19 | the estimated IQR implicitly captures climate simulation and downscaling uncertainties, in  
20 | addition to explicitly representing model parameter uncertainty. The need to consider  
21 | uncertainties at each and every step of the process starting with, for example, downscaling  
22 | methods (statistical, dynamical or some combination of statistical and dynamical methods) is  
23 | a topic of ongoing research.

## 24 | **4.2 Hydrologic and GEV model validation**

25 | ~~Since~~Because we ~~used~~utilize ~~modeled~~modelled VIC flows for flood analysis, there are two  
26 | considerations for model validation. First, we compare VIC simulated one day flood events to  
27 | the observed unregulated flow estimates (i.e. validating that our calibrated VIC model is  
28 | accurately simulating flood flows). Second, we compare the GEV ~~modeled~~modelled floods to  
29 | the VIC simulated ~~flows~~one day flood events and the observed unregulated flow estimates  
30 | (i.e. validating that the GEV models we fit to the simulated data match both the observed  
31 | unregulated flows and the VIC simulated flows).

1 Although, unregulated flows are not available for the entire period of record, one-day  
2 maximum unregulated flow estimates are available at Reno for six historical floods [USACE,  
3 2013b]. Figure 3 plots the observed flow (blue triangle) with the one-day VIC flow that was  
4 simulated using historical observed forcings from Maurer et al. [2002] (red triangle), and a  
5 boxplot of the non-stationary GEV distribution for the same month generated using the same  
6 monthly historical precipitation and temperature [i.e. Maurer et al., 2002]. Comparing first  
7 the one day maximum VIC simulated flow with the observed flow the maximum percent  
8 difference between the natural logarithm of simulated and observed flows is 12%. There does  
9 appear to be a slight positive bias in the VIC simulations (i.e. VIC simulated flows are greater  
10 than observed flood flows). Still, the simulated flood values (red circles) generally fall within  
11 the interquartile range of the GEV distribution, except in the case of the February 2, 1963  
12 flood and the January 2, 1997 flood.

13 In these instances the VIC simulation matches very closely (percent difference in the natural  
14 logarithm of flows are 0.5% and 1.2% respectively) with the observed flow, however, the  
15 GEV model underestimates the events. This discrepancy is caused by the flood timing. In  
16 both cases the flood occurs at the very beginning of the month. In the GEV framework,  
17 precipitation and temperature are used as covariates for the flow of the same month. However,  
18 for these storms, flooding is linked to precipitation and temperature in the month of flooding  
19 and the preceding month. Therefore, the GEV model simulates the flood in the preceding  
20 month and/or underestimates the flood magnitude if the precipitation is split between two  
21 months. While this is a limitation for matching individual historical events, primarily timing,  
22 it ~~should~~is not ~~be~~ a major concern ~~for~~ future projections. This is because, for the purposes  
23 of risk calculations, it really doesn't matter in which month the GEV model simulates the  
24 flood event as long as it realistically captures flood magnitude behaviour.

25 Comparing the GEV model distribution to the other observed floods (blue triangles), the  
26 distribution encompasses the observed flood magnitude (within the 5th and 95th percentile)  
27 for all except for two of the floods (1955 and 1963). For 1963, the VIC simulated and  
28 observed floods are in close agreement (the difference between the natural logarithm of  
29 simulated and observed flows is the smallest of any event at 0.5%) and the discrepancy with  
30 the GEV model is consistent with the flood timing described above. The 1955 flood resulted  
31 from 38 cm of melted snow combined with 33 cm of rainfall over a three day period [O'Hara  
32 et al., 2007]. In the historical forcings used to drive the VIC model December 1955 has 75 cm

1 of precipitation which is the highest December precipitation value in the historical period. In  
2 this instance, the VIC simulated flow falls within the interquartile range of the GEV model,  
3 but the high monthly precipitation results in an overestimation of the flood magnitude.  
4 Again, this is a limitation of using monthly forcings because the total December precipitation  
5 is used as a covariate and not a storm specific value though in many cases the storm specific  
6 values constitute the bulk of the monthly precipitation totals.

7 Figure 4 is a time series plot of VIC historical simulated flow along with the median and 5th  
8 to 95th percentile flow of the GEV model. As would be expected from the model fit  
9 demonstrated in Figures 2 and 3, Figure 4 shows that the VIC simulated flows are generally  
10 close to the median GEV ~~modeled~~ modelled flow and nearly always fall within the 5th to 95th  
11 percentile range. Although there are differences in the simulation of individual events  
12 discussed above, the median simulated flood magnitudes are only greater than the maximum  
13 observed flood in two instances [of the 300 historical months simulated](#).

14 In general, Figures 3 and 4 show that the VIC simulated flows match closely with the  
15 observed floods (based on percent difference in the natural logarithm of flows) and that the  
16 interquartile range of the GEV distributions encompass the observed and simulated flows in  
17 most instances. Figure 3 does illustrate some of the complications in matching individual  
18 events. However, based on analysis of the driving forces behind each individual event we  
19 are able to [explain and](#) document the sources of these discrepancies. Based on this analysis we  
20 conclude that the [VIC](#) model behaviour [has](#) a reasonable match with the natural system.

21

### 22 4.3 Future flood risk

23 Future flood risk is calculated using [Equation \(5b\)](#) from Table 1. For the first part of this  
24 analysis we define ‘flood’ as one-day flow exceeding 1,065 cms (37,600 cfs). This is the  
25 maximum historical unregulated flow at Reno from the January 2, 1997 event and is  
26 considered to be the design flood for flood protection infrastructure design. For each  
27 simulation month (1950-2099 November –April) exceedance probabilities are calculated for  
28 every climate projection (234 in total) using the selected non-stationary GEV models from  
29 Table 3 (fit to the historical observations) and the projected monthly precipitation and  
30 temperature. As detailed in the section 3.2, when exceedance probabilities are time dependent,  
31 the flood risk (refer to equation 5b, Table 1) is a function of both the length of the design life

1 and the period of operation. Figure 5 plots the risk of flood versus project life for three time  
2 periods, 1950 to 1999, 2000 to 2049 and 2050 to 2099. In other words, this is the risk of a  
3 flood exceeding 1,065 cms in the next  $n$  years if you are standing in 1950, 2000 or 2050. The  
4 median and interquartile ranges show the distribution of the 234 climate projections  
5 simulated. Here we use the interquartile range, as opposed to the 5th and 95th percentile, to  
6 focus on the central tendencies of each time period ~~and not the variability between~~  
7 ~~projections~~. Note that the ranges presented here express the variability between climate  
8 ~~projections~~models. Uncertainty of ~~future the~~ VIC model ~~simulations~~ is not investigated  
9 ~~directly~~ here. For ~~a more~~ detailed analysis of ~~an~~ uncertainty in VIC simulations the reader is  
10 referred to Elsner et al. [2014].

11 For both Farad and Reno there is a clear positive shift in flood risk between the three time  
12 periods. In all cases the median risk for each subsequent time period falls outside the  
13 interquartile range of the preceding time period although the prediction spread for Reno is  
14 greater than Farad. It is important to note that the flood risk is actually higher at Farad than  
15 Reno in both the historical and future periods despite the fact that the observed flow  
16 distributions at the two stations are very similar (refer to Figure2). This shift between Farad  
17 and Reno is caused by the differences in the shape parameters (refer to Table 3). Farad has a  
18 ~~relatively~~ heavier tailed distribution (~~i.e., the GEV shape parameter for Farad is greater than~~  
19 ~~the shape parameter for Reno~~) and therefore flood risks are increased. The sensitivity of the  
20 model parameters (and the associated flood risk) to small differences in the flow and covariate  
21 distributions is further demonstrated by Figure 6.

22 Figure 6 presents the project life risk from Figure 5 for three project life periods (10, 20 and  
23 30 years). Boxplots show the non-stationary model results for the 234 climate projections  
24 with the different time periods compared side by side. Also, the risk calculated using a  
25 stationary GEV model and a stationary LP3 model (i.e. the distribution prescribed by Bulletin  
26 17B ~~and fitted~~ using ~~the~~ L-moments [IACWD, 1982]) fit to the historical flow data are plotted  
27 for reference (blue and red dashed lines respectively). Comparing between these three  
28 approaches (non-stationary GEV, stationary GEV and stationary LP3) provides information  
29 on the sensitivity of results to ~~modell~~ing approach and non-stationary parameters. For  
30 instance, both stationary models are fit to the same historical simulated flows (one using MLE  
31 and the other using L-moments) so differences between the stationary lines reflect the impact  
32 of model choice and fitting approach on estimated risk. Conversely the stationary GEV

1 model (blue line) and the historical non-stationary models (grey boxplot) have the same  
2 model form and cover the same time period; the only difference is the addition of covariates  
3 to estimate model parameters. Thus differences between these two show the effect of model  
4 parameter changes from the non-stationary approach. Finally, variability between the  
5 boxplots for a given design period demonstrates the evolution of risk over time (i.e. the  
6 impact of climate ~~changetrends~~ on risk). The latter (i.e. changing risk over time), is the  
7 purpose of this analysis, however before assessing ~~changetrends~~ over time we must first  
8 discuss the impact of model choice and parameters on risk estimates.

9 For both of the stationary methods, the risk increases with project life following equation (5a)  
10 from Table 1. The distinction between these lines and the non-stationary approaches is that,  
11 with the stationary approach, a single exceedance probability is calculated for the given flood  
12 magnitude and this probability is assumed to remain constant throughout the design life. Also,  
13 for both stationary approaches the model is fit directly to the historical one day maximum  
14 flow distribution and no covariates are required (note that stationary models are not fit to the  
15 future time periods because this would require future simulated flows). -Comparing between  
16 the GEV (blue line) and the LP3 (red line) stationary models there is a 10-20% increase in  
17 risk between the two models. This difference is purely a function of model form and  
18 highlights the sensitivity of the risk calculations to model choice.

19 Contrasting the difference between the stationary (blue line) and the non-stationary GEV for  
20 the historical time period (grey boxplot) illustrates the effect of adding non-stationary  
21 parameters to a given model form. Recall that in both cases the GEV model is fit to the  
22 historical simulated flows. However, for the stationary approach, model fitting results in a  
23 single set of parameters (location, scale and shape) whereas with the non-stationary approach  
24 we derive the shape parameter and a set of coefficients for linear models to determine the  
25 location and scale parameters based on precipitation and temperature values. Thus, for the  
26 non-stationary approach, different location and scale parameters are calculated for every  
27 historical cool season month and GCM model (234).

28 Overall, there is close agreement between the stationary (S) and average non-stationary (NS)  
29 location parameters (6.55 S vs. 6.64 NS at Farad and 6.63 S vs. 6.78 NS at Reno). However,  
30 for both gauges the scale parameter is lower with the non-stationary approach (1.30 S vs. 0.94  
31 NS at Farad and 1.28 S vs. 0.96 NS at Reno). At Reno the shape parameter is similar (-0.24 S  
32 vs. -0.27 NS), but at Farad the difference is somewhat larger (-0.24 S vs. -0.18 NS).

1 Differences in model parameters are reflected in the distance between the stationary GEV  
2 model (blue line) and the median historical non-stationary GEV boxplots (~~center~~centre of the  
3 grey boxplots) in Figure 6. For Reno, the stationary line is closer to the historical boxplots.  
4 However, at Farad, the non-stationary boxplots are consistently higher than the stationary  
5 line. The larger differences between the stationary and non-stationary models for Farad result  
6 from changes in the shape parameter between the stationary and non-stationary model fits.  
7 This change demonstrates the sensitivity of model results to changes in model parameters.

8 As with Figure 5, Figure 6 shows significant increases in risk moving into the future and  
9 subsequently larger differences between the stationary and non-stationary approach. By the  
10 second future period the differences between the stationary and non-stationary models can be  
11 as much as 50% or more. For both gauges difference in risk between the non-stationary and  
12 stationary approaches grows over time, indicating greater potential to underestimate risk  
13 looking further into the future if non-stationary parameters are not ~~considered~~adopted.

14 ~~Although the figures are not shown here,~~ Results were also grouped by RCPs to  
15 ~~analyze~~analyze connections between greenhouse gas emission rates and changes in flood risk.  
16 ~~As shown in Figure 7,~~ We observed no clear trend in flood risk based on the different RCPs.  
17 This indicates that, ~~for this flood statistic in this basin,~~ the variability between GCM model  
18 form and initial conditions likely overwhelms the influence of greenhouse gas emissions  
19 when comparing between scenarios. ~~Although we caution that this is not a general finding, for~~  
20 ~~this application, we show that~~ ~~In other words,~~ the variability between projections within any  
21 RCP scenario is larger than the difference between RCP scenarios. ~~Harding et al. [2012] also~~  
22 ~~noted similar behaviour in their study of the Colorado River Basin.~~

23 Given the sensitivity of projected risk to model parameters, an obvious question is whether  
24 increases in risk over time are similarly sensitive. For the 1,065 cms flood plotted in Figure 6,  
25 the increased risk with added project life (i.e. 20 years vs. 10 years) is greater with the non-  
26 stationary models than the stationary one at both stations. This is intuitive, given the increased  
27 flood risk with time demonstrated in Figure 5 for the non-stationary models. Although, Farad  
28 has higher ~~overall risk~~overall, the relative increase in risk between time periods is similar  
29 between the two stations. For example, the median ten year flood risk increases by 21% for  
30 Farad comparing between the first (1950-1999) and second (2000-2049) time periods  
31 compared to 29% for Reno.

1 | Next, analysis is expanded to a range of flood magnitudes. Figure 7-8 plots the flood risk over  
2 | a ten year project life starting in 1950, 2000, and 2050 for flood values ranging from 283 to  
3 | 1,416 cms (10,000 to 50,000 cfs). As would be expected the ten year flood risk decreases  
4 | with increasing flood rate. The shapes of the curves are slightly different between Farad and  
5 | Reno; flood risk decreases more sharply with increased flow at Reno than Farad. Again this  
6 | behaviour is a function of the shape parameter of the respective GEV distributions. Despite  
7 | these differences, both gauges display clear shifts between time periods similar to Figure 5.  
8 | Here again, the median risk for each subsequent period consistently falls outside the  
9 | interquartile range of the preceding period.

10 | Changes in the median flood risk (i.e. differences between the solid lines on Figure 7-8)  
11 | between each future period and the historical period are plotted in Figure 8-9 for both gauges.  
12 | As would be expected based on the qualitative differences in Figure 7-8, the shape of the Farad  
13 | and Reno difference curves are slightly different. However, the salient point for this analysis  
14 | is that the increased risk between periods is generally within 10% between the two stations.  
15 | Overall the increased risk between the first future period (2000-2050) and the historical  
16 | period (1950-1999) is between 10 and 20% for flows from 600 to 1,200 cms-. Similarly, the  
17 | increased risk from the historical period to the second future period (2050-2099) is between  
18 | 30 and 50%. Differences for the highest and lowest flows are difficult to assess because the  
19 | median is skewed for high and low flow values by the fact that the risk values are bound  
20 | between 0 and 100 percent. upper and lower limits of risk (i.e. 0 and 100%).

21

## 22 | 5 Summary and Conclusions

23 | The analysis presented is unique in its incorporation of non-stationary GEV analysis using  
24 | CMIP-5 projections and the design life level risk assessment concepts. We present our  
25 | findings as a relevant case study and an example application of recent developments in non-  
26 | stationary flood assessment. Lacking sufficient unregulated flow data we simulate historical  
27 | floods using the VIC model. Subsequently we use the simulated floods to fit non-stationary  
28 | GEV models with downscaled monthly precipitation and temperature as covariates. Although  
29 | there are some discrepancies between individual simulated and observed flood events, we  
30 | demonstrate that the VIC model adequately captures the range of flood magnitudes.  
31 | Furthermore, we show that that the GEV modelled historical floods are in good agreement  
32 | with both the VIC simulated floods and the published flood events [USACE, 2013b].

Formatted: Font: Not Italic



1 Discrepancies between historical and simulated events often result from the monthly time step  
2 used for covariates. This can affect the ability to model floods that are generated by  
3 precipitation that occurs in two months. Also, because the climate variables are monthly  
4 aggregates, and not event based, large floods can be generated in months with high  
5 precipitation even if that precipitation does not occur in one concentrated event. – Despite  
6 these differences, comparison with historical flood events demonstrates that the GEV model  
7 does reasonably well in a good job of encompassing at simulating historical flood magnitudes,  
8 even if some individual historical events are not matched exactly.

9 Using the derived non-stationary GEV models, we generate flood distributions for 234  
10 CMIP5 climate projections from 1950 to 2099. For the historical one-day design flood  
11 magnitude of 1,065 cms, results show significant increases in the frequency of high flow  
12 events in the future. From a water management standpoint this finding translates directly to  
13 increased flood risk. For example, we calculate a 21% (29%) increase risk of a 1,065 cms  
14 flood over a 10 year design life for Farad (Reno) from the historical time period to the first  
15 future period, and similar increases from the first future period to the second. Increased risk  
16 between time periods is also relatively consistent for longer design life periods and similar  
17 shifts in flood risk are noted across a range of flood magnitudes. For both stations the  
18 increased risk from the historical to the first future period is between 10 and 20% and from  
19 the historical to the second future period is between 30 and 50% for floods ranging from 600  
20 to 1,200 cms.

21 The significant increases in flood risk through time indicate the importance of non-stationary  
22 flood frequency analysis for future infrastructure planning and the potential to underestimate  
23 risk when stationarity is assumed. For both stations the difference between the stationary and  
24 non-stationary approach increases over time. By the second future period (2000-2049),  
25 differences in risk calculations between the stationary and non-stationary models can be 50%  
26 or larger. This finding is in keeping with a number of recent studies [e.g. Griffis and  
27 Stedinger, 2007; Katz et al., 2002; Towler et al., 2010] that have highlighted potential  
28 applications for non-stationary analysis of flood frequency.

29 An important consideration for this approach is the sensitivity of results to model parameters.  
30 In all cases the flood risk is higher at Farad than Reno due to the relatively heavier tailed  
31 distribution that was fit. Estimated model parameters differed by station despite the fact that  
32 the flow, precipitation and temperature distributions for both locations are very similar.

Formatted: Font: Not Italic

Formatted: Font: Not Italic

Formatted: Font: Not Italic

1 While these changes effected the overall risk projections the relative increase in risk over time  
2 remained consistent between stations. This indicates that the more robust metric from this  
3 analysis is the relative increase in flood risk and not the absolute values. This finding is  
4 further supported by the fact that absolute flood risk estimates could be impacted by model  
5 bias. By focusing on differences in risk we specifically highlight the impact of non-  
6 stationarity on risk assessment, as opposed to parameter sensitivity. Similarly, it is important  
7 to note that this analysis is based on natural flow estimates and does not include infrastructure  
8 development or operation, ~~and results~~ ~~As such results~~ indicate the potential increase in the  
9 underlying natural flood risk ~~in the UTRB over the 21<sup>st</sup> century, and not the potential increase~~  
10 ~~in flood damages.~~

Formatted: Superscript

11

## 12 **Acknowledgement**

Formatted: Font: Bold

13 The authors would like to acknowledge the WaterSMART Basin Study program for  
14 funding the Truckee River Basin Study which supported this research. In addition we  
15 would like to thank the reviewers for their constructive comments that helped to  
16 improve the manuscript.

Formatted: Left

## 1 **References**

- 2 Akaike, H. (1974), New look at statistical-model identification, *IEEE Trans. Autom. Control*,  
3 *19*, 716-723.
- 4 Allan, R. P. (2011), Climate change: Human influence on rainfall, *Nature*, *470*, 344-345.
- 5 Cayan, D. R., K. T. Redmond, and L. G. Riddle (1999), ENSO and Hydrologic Extremes in  
6 the Western United States, *Journal of Climate*, *12*(2881-2893).
- 7 Cayan, D. R., S. A. Kammerdiener, M. D. Dettinger, J. M. Caprio, and D. H. Peterson (2001),  
8 Changes in the Onset of Spring in the Western U.S., *Bulletin of the American*  
9 *Meteorological Society*, *82*(3), 399-415.
- 10 Christensen, N. S., and D. P. Lettenmaier (2007), A multimodel ensemble approach to  
11 assessment of climate change impacts on the hydrology and water resources of the Colorado  
12 River Basin, *Hydrology and Earth System Science*, *11*, 1417-1434.
- 13 Christensen, N. S., A. W. Wood, D. P. Lettenmaier, and R. N. Palmer (2004), Effects of  
14 climate change on the hydrology and water resources of the Colorado river basin, *Climate*  
15 *Change*, *62*(103), 337-363.
- 16 Das, T., D. W. Pierce, D. R. Cayan, J. A. Vano, and D. P. Lettenmaier (2011), The  
17 importance of warm season warming to western U.S. streamflow changes, *Geophysical*  
18 *Research Letters*, *38*(L23403).
- 19 Dettinger, M. D., and D. R. Cayan (1995), Large-scale Atmospheric Forcing of Recent Trends  
20 toward Early Snowmelt Runoff in California, *Journal of Climate*, *8*(3), 606-623.
- 21 Douglas, E. M., R. M. Vogel, and C. N. Kroll (2000), Trends in floods and low flows in the  
22 United States: impact of spatial correlation, *Journal of Hydrology*, *240*(1-2), 90-105.
- 23 Easterling, D. R., G. A. Meehl, C. Parmesan, S. A. Changnon, T. R. Karl, and L. O. Mearns  
24 (2000), Climate Extremes: Observations, Modeling and Impacts, *Science*, *289*(5487), 2068-  
25 2074.
- 26 Elsner, M. M., S. G. Gangopadhyay, T. Pruitt, L. D. Brekke, N. Mizukami and M. P. Clark  
27 (2014), How does the choice of distributed meteorological data affect hydrologic model  
28 calibration and streamflow simulations?, *Journal of Hydrometeorology*, *15*, 1384-1403.

1 Franks, S. W. (2002), Identification of a change in climate state using regional flood data,  
2 *Hydrol. Earth Syst. Sci.*, 6, 11-16.

3 Gangopadhyay, S., T. Pruitt, L. D. Brekke, and D. A. Raff (2011), Hydrologic Projections for  
4 the Western United States, *EOS*, 92(48), 441-452.

5 Gilleland, E., and R. W. Katz (2011), New software to analyze how extremes change over  
6 time. , *Eos* 92(2), 13-14.

7 Gilroy, K. L., and R. H. McCuen (2012), A nonstationary flood frequency analysis method to  
8 adjust for future climate change and urbanization, *Journal of Hydrology*, 414-415, 40-48.

9 Griffis, V., and J. R. Stedinger (2007), Incorporating climate change and variability into  
10 Bulletin 17B LP3 model, paper presented at ASCE World Env. & Water Resour. Congress.

11 Gutowski, W. J., G. C. Hegerl, G. J. Holland, T. R. Knutson, L. O. Mearns, R. J. Stouffer, P.  
12 J. Webster, M. F. Wehner, and F. W. Zwiers (2008), Causes of Observed Changes in  
13 Extremes and Projections of Future Changes in Weather and Climate Extremes in a Changing  
14 Climate. Regions of Focus: North America, Hawaii, Caribbean, and U.S. Pacific Islands *Rep.*,  
15 Washington, DC.

16 [Hall, J., B. Arheimer, M. Borga, R. Brázdil, P. Claps, A. Kiss, T. R. Kjeldsen,](#)  
17 [J. Kriaučiūnienė, Z. W. Kundzewicz, M. Lang, M. C. Llasat, N. Macdonald, N. McIntyre,](#)  
18 [L. Mediero, B. Merz, R. Merz, P. Molnar, A. Montanari, C. Neuhold, J. Parajka,](#)  
19 [R. A. P. Perdigão, L. Plavcová, M. Rogger, J. L. Salinas, E. Sauquet, C. Schär, J. Szolgay,](#)  
20 [A. Viglione, and G. Blöschl et al.](#) (2014), Understanding flood regime change in Europe: a  
21 state-of-the-art assessment, *Hydrol. Earth Syst. Sci.*, 18, 2735-2772.

22 [Harding, B.L., A.W. Wood and J.R. Prairie \(2012\), The implications of climate change](#)  
23 [scenario selection for future streamflow projection in the Upper Colorado River Basin,](#)  
24 [Hydrol. Earth Syst. Sci. 16, 3989-4007.](#)

25 Hirsch, R. M. (2011), A perspective on nonstationarity and water management, *Journal of the*  
26 *American Water Resources Association*, 47(3), 436-446.

27 Interagency Advisory Committee on Water Data (IACWD) (1982), Guidelines for  
28 determining flood flow frequency: Bulletin 17B of the Hydrology Subcommittee, Office of  
29 Water Data Coordination, U.S. Geological Survey, Reston, VA., 183 p.

1 Jain, S., and U. Lall (2001), Floods in a changing climate: Does the past represent the future?,  
2 *Water Resources Research*, 37(12), 3193-3205.

3 Katz, R. W. (2010), Statistics of extremes in climate change, *Climate Change*, 100, 71-76.

4 Katz, R. W., M. B. Parlange, and P. Naveau (2002), Statistics of extremes in hydrology,  
5 *Advances in Water Resources*, 25, 1287-1304.

6 Kunkel, K. E. (2003), North American Trends in Extreme Precipitation, *Natural Hazards*, 29,  
7 291-305.

8 Liang, X., E. F. Wood, and D. P. Lettenmaier (1996), Surface soil moisture parameterization  
9 of the VIC-2L model: Evaluation and modification, *Global and Planetary Change*, 13(1-4),  
10 195-206.

11 Liang, X., D. P. Lettenmaier, E. F. Wood, and S. J. Burges (1994), A simple hydrologically  
12 based model of land surface water and energy fluxes for general circulation models, *Journal*  
13 *of Geophysical Research*, 99(D7), 14415-14428.

14 Madsen, T., and E. Figdor (2007), When it Rains it Pours - Global Warming and the Rising  
15 Frequency of Extreme Precipitation in the U.S., edited, Environmental America Research and  
16 Policy Center.

17 Maidment, D. R. (1993), *Handbook of Hydrology*, McGraw-Hill, ISBN 0070397325.

18 Mailhot, A. and S. Duchesne (2010), Design criteria of urban drainage infrastructures under  
19 climate change, *Journal of Water Resources Planning and Management*, 136(2), 201-208.

20 Maurer, E. P., L. D. Brekke, T. Pruitt, and P. B. Duffy (2007), Fine-resolution climate  
21 projections enhance regional climate change impact studies, *Eos Tran. AGU*, 88(47), 504.

22 Maurer, E. P., A. W. Wood, J. C. Adam, D. P. Lettenmaier, and B. Nijssen (2002), A Long-  
23 Term Hydrologically-Based Dataset of Land Surface Fluxes and States for the Conterminous  
24 United States, *Journal of Climate*, 15(22), 3237-3252.

25 Meehl, G. A., [T. Karl](#), [D. R. Easterling](#), [S. Changnon](#), [R. Pielke Jr.](#), [D. Changnon](#), [J. Evans](#), [P.](#)  
26 [Ya Grouisman](#), [T. R. Knutson](#), [K. E. Kunkel](#), [L. O. Mearns](#), [C. Parmesan](#), [R. Pulwarty](#), [T. Root](#),  
27 [R. T. Sylves](#), [P. Whetton](#), and [F. Zwiers](#) (2000), An Introduction to Trends in Extreme  
28 Weather and Climate Events: Observations, Socioeconomic Impact, Terrestrial Ecological  
29 Impacts, and Model Projections, *Bulletin of the American Meteorological Society*, 81, 413-  
30 416.

1 Merz, B., S. Vorogushyn, S. Uhlemann, J. Delgado and Y. Hundecha (2012), More efforts  
2 and scientific rigour are needed to attribute trends in flood time series, *Hydrol. Earth Syst.*  
3 *Sci. Opinions*, 16, 1379-1387.

4 Milly, P. C. D., J. Betancourt, M. Falkenmark, R. M. Hirsch, Z. W. Kundzewicz, D. P.  
5 Lettenmaier, and R. J. Stouffer (2008), Stationarity Is Dead: Whither Water Management,  
6 *Science*, 319(5863), 573-574.

7 Min, S.-K., X. Zhang, F. W. Zwiers, and G. C. Hegerl (2011), Human contribution to more-  
8 intense precipitation extremes, *Nature* 470, 378-381.

9 Mote, P.W., A.F. Hamlet, M.P. Clark, And D.P. Lettenmaier (2005), Declining Mountain  
10 Snowpack In Western North America, *Bulletin of the American Meteorological Society*, 39-  
11 49, doi: 10.1175/BAMS-86-1-39.

12 Mullet, C. J., P. A. O’Gorman, and L. E. Back (2011), Intensification of precipitation  
13 extremes with warming in a cloud resolving model, *Journal of Climate*, 24(2784-2800).

14 Nijssen, B., D. P. Lettenmaier, X. Liang, S. W. Wetzel, and E. F. Wood (1997), Streamflow  
15 simulation for continental-scale river basins, *Water Resources Research*, 33(4), 711-724.

16 Obeysekera, J. and J. D. Salas (2014), Quantifying the uncertainty of design floods under  
17 nonstationary conditions, *Journal fo Hydrologic Engineering*, 19, 1438-1446.

18 O’Gorman, P. A., and T. Schneider (2009), The physical basis for increases in precipitaiton  
19 extremes in simulations of 21st century climate change, *Proceedings of hte National Academy*  
20 *of Sciences*, 106, 14773-14777.

21 O’Hara, B.F., G.E. Barbato, J.W. James, H.A. Angeloff and T. Cylke (2007), ‘Weather and  
22 climate of the Redno-Carson City- Lake Tahoe Region, Nevada Bureau of Mines and  
23 Geology, Special Publication 34.

24 Pall, P., T. Aina, D. A. Stone, P. A. Stott, T. Nozawa, A. G. J. Hilberts, D. Lohmann, and M.  
25 R. Allen (2011), Anthropogenic greenhouse gas contribution to flood risk in England and  
26 Wales in autumn 2000, *Nature*, 470, 382-385.

27 Payne, J. T., A. W. Wood, A. F. Hamlet, R. N. Palmer, and D. P. Lettenmaier (2004),  
28 Mitigating the effects of climate change on the water resources of the Columbia River basin,  
29 *Climate Change*, 62(1-3), 233-256.

1 [Pierce, D. W., T. P. Barnett, B. D. Santer and P. J. Gleckler \(2009\), \*Selecting global climate\*](#)  
2 [models for regional climate change studies, \*PNAS\*, 106\(21\), 8441-8446.](#)

3 Pierce, D. W., T. Das, D. R. Cayan, E. P. Maurer, N. L. Miller, Y. Bao, M. Kanamitsu, K.  
4 Yoshimura, M. A. Snyder, L. C. Sloan, G. Franco, M. Tyree (2012), Probabilistic estimates of  
5 future changes in California temperature and precipitation using statistical and dynamical  
6 downscaling, *Climate Dynamics*, 40, 839-856.

7 Raff, D. A., T. Pruitt, and L. D. Brekke (2009), A framework for assessing flood frequency  
8 based on climate projection information, *Hydrol. Earth Syst. Sci.*, 13, 2119-2136.

9 Ralph, F. M., and M. D. Dettinger (2012), Historical and National Perspectives on Extreme  
10 West Coast Precipitation Associated with Atmospheric Rivers during December 2010,  
11 *Bulletin of the American Meteorological Society*(June), 783-790.

12 [R Core Team \(2012\). \*R: A language and environment for statistical computing\*. R Foundation](#)  
13 [for Statistical Computing, Vienna, Austria. ISBN 3-900051-07-0. URL \[http://www.R-\]\(http://www.R-project.org/\)](#)  
14 [project.org/.](#)

15 Reclamation (2010), Truckee River Basin Study, Fact Sheet, available at  
16 [http://www.usbr.gov/WaterSMART/bsp/docs/fy2010/Truckee\\_Basin\\_Factsheet\\_Final.pdf](http://www.usbr.gov/WaterSMART/bsp/docs/fy2010/Truckee_Basin_Factsheet_Final.pdf).

17 Reclamation (2011), West-wide climate risk assessments: Bias-corrected and spatially  
18 downscaled surface water projections, Tech. Memo., 86-68210-2011-01, 138 pp., Tech. Serv.  
19 Cent., U.S. Dep. of the Inter., Denver Colo., March.

20 Reclamation (2013). Downscaled CMIP3 and CMIP5 Climate Projections: Release of  
21 Downscaled CMIP5 Climate Projections, Comparison with Preceding Information, and  
22 Summary of User Needs. Downscaled CMIP3 and CMIP5 Climate and Hydrology  
23 Projections. U.S. Department of the Interior, Bureau of Reclamation, Technical Service  
24 Center, Denver, Colorado, 116 p.

25 Reclamation (2014), 'Downscaled CMIP3 and CMIP5 Climate and Hydrology Projections:  
26 Release of Hydrology Projections, Comparison with preceding Information, and Summary of  
27 User Needs', prepared by the U.S. Department of the Interior, Bureau of Reclamation,  
28 Technical Services Center, Denver, Colorado. 110 pp.

29 Regonda, S. K., B. Rajagopalan, M. Clark, and J. Pitlick (2005), Seasonal Cycle Shifts in  
30 Hydroclimatology Over the Western U.S., *Journal of Climate*, 18(2), 372-384.

1 Rootzén, H., and R. W. Katz (2013), Design Life Level: Quantifying risk in a changing  
2 climate, *Water Resources Research*, 49, 5964-5972.

3 Salas, J., and J. Obeysekera (2014), Revisiting the Concepts of Return Period and Risk for  
4 Nonstationary Hydrologic Extreme Events, *Journal of Hyrol. Eng.*, 19(3), 554-568.

5 Slack, J.R., A.M. Lumb, and J.M. Landwehr (1993). 'Hydroclimatic data network (HCDN): A  
6 U.S. Geological Survey streamflow data set for the United Sates for the study of climate  
7 variation, 1874-1988,' *USGS Water Resour. Invest. Rep.*, 93-4076.

8 Small, D., S. Islam, and R. M. Vogel (2006), Trends in precipitation and streamflow in the  
9 eastern U.S.: Paradox or perception? *Geophysical Research Letters*, 2006(3).

10 Stedinger, J. R. and V. W. Griffis (2011), Getting from here to where? Flood frequency  
11 analysis and climate, *Journal of the American Water Resources Association*, 47(3), 506-513.

12 Stokes, J. (2002), Draft Farad Diversion Dam Replacement Project Environmental Impact  
13 Report *Rep.*, State Water Resources Control Board, Sacramento, CA.

14 Sun, Y., S. Solomon, A. Dai, and R. W. Portmann (2007), How Often Will it Rain?, *Journal*  
15 *of Climate*, 20, 4801-4818.

16 Taylor, K. E., Stouffer, R. J. & Meehl, G. A. (2012), A Summary of the CMIP5 Experiment  
17 Design. *Bull. Am. Meteorol. Soc.* 93, 485-498.

18 Towler, E., B. Rajagopalan, E. Gilleland, R. S. Summers, D. Yates, and R. W. Katz (2010),  
19 Modeling hydrologic and water quality extremes in a changing climate: A statistical approach  
20 based on extreme value theory, *Water Resources Research*, 46(W11504).

21 USACE (2013a), Final environmental impact statement for the Truckee Meadows Flood  
22 Control Project: General Reevaluation Report Volume 1. US Army Corps of Engineers,  
23 Sacramento.

24 USACE (2013b), Truckee Meadows Flood Control Project, Nevada: Draft General  
25 Reevaluation Report *Rep.*, US Army Corps of Engineers, Sacramento.

26 Van Rheezen, N. T., A. W. Wood, R. N. Palmer, and D. P. Lettenmaier (2004), Potential  
27 implications of PCM climate change scenarios for Sacramento-San Joaquin River Basin  
28 hydrology and water resources, *Climate Change*, 62(1-3), 257-281.



- 1 Villarini, G., F. Serinaldi, J. A. Smith, and W. F. Krajewski (2009), On the stationarity of  
2 annual flood peaks in the continental United States during the 20th century, *Water Resources*  
3 *Research*, 45(8).
- 4 Vogel, R. M., C. Yaindl, and M. Walter (2011), Nonstationarity: Flood magnification and  
5 recurrence reduction factors in the United States, *JAWRA*, 47(3), 464-474.
- 6 Walter, M., and R. M. Vogel (2010), Increasing trends in peak flows in the northeastern  
7 United States and their impacts on design, paper presented at 2nd Joint Federal Interagency  
8 Conference, Las Vegas, NV.
- 9 Wood, A. W., Leung, L. S. R., Sridhar, V., and Lettenmaier, D. P. (2004), Hydrologic  
10 implications of dynamical and statistical approaches to downscaling climate model outputs,  
11 *Climatic Change*, 62, 189–216.
- 12 | Wu, H., R. F. Adler, Y. Tian, G. J. Juffman, H. Li and J. J. Wang ([In press 2014](#)), Real-time  
13 | global flood estimation using satellite-based precipitation and a coupled land surface routing  
14 | model, *Water Resources Research*, [50\(3\), 2693-2717](#).
- 15

1 **Table 1: Flood calculations using stationary and non-stationary distributions (adapted**  
 2 **from Salas and Obeysekera [2014])**

Eqn. #	Description	a. Stationary	b. Non Stationary
1	Exceedance probability (Probability of flood <sup>1</sup> occurring in year $x$ )	$p$	$p_x$
2	Probability of the first flood occurring in year $x$ <sup>2</sup>	$f(x) = (1 - p)^{x-1}p$	$f(x) = p_x \prod_{t=1}^{x-1} (1 - p_t)$
3	Probability of a flood occurring before year $x$ <sup>3</sup>	$F(x) = \sum_{i=1}^x f(i)$	
		$F(x) = 1 - (1 - p)^x$	$F(x) = 1 - \prod_{t=1}^x (1 - p_t)$
4	Return Period (Expected waiting time between flood occurrences <sup>4,5</sup> )	$E(X) = \sum_{x=1}^{\infty} x * P(X = x)$	
		$E(X) = 1/p$	$E(X) = 1 + \sum_{x=1}^{x_{max}} \prod_{t=1}^x (1 - p_t)$
5	Probability of a flood occurring before the design life $n$ <sup>6</sup>	$R = P(X \leq n) = F(n)$	
		$R = 1 - (1 - p)^n$	$R = 1 - \prod_{t=1}^n (1 - p_t)$

3

4 <sup>1</sup> Flood is defined as a flow exceeding a predefined threshold

5 <sup>2</sup>  $f(x)$  = Probability density function of  $X$

6 <sup>3</sup>  $F(x)$  = Cumulative distribution function of  $X$

7 <sup>4</sup>  $X$  = Random variable denoting the waiting time for the first flood occurrence

8 <sup>5</sup>  $x_{max}$  = Time when  $p_x$  equals 1

9 <sup>6</sup>  $n$  = The length of the time period over which flood risk is calculated

10

11

1  
2 Table 2: Negative log likelihood(NLLH) and Akaike information Criterion (AIC) scores  
3 for each model, as well as the deviance statistics (D) of pairwise comparisons of  
4 different model configurations (P = precipitation only, T= temperature only P&T= both)  
5 and the p-values of each D score based on a chi-squared distribution. The number of  
6 parameters in each model and the models used for comparison are listed at the bottom  
7 of the table. The selected model for each station is shaded in grey.

Station	Metric	Stationary 1	Non stationary Location			Non stationary Scale			Non stationary Location and		
			P & T 2	P 3	T 4	P & T 5	P 6	T 7	P & T 8	P 9	T 10
Farad	NLLH	508.9	422.9	467.1	499.7	487.3	500.9	506.5	416.4	462.2	496.9
	AIC	1023.7	855.9	942.3	1007.4	984.6	1009.8	1021.1	846.8	934.4	1003.8
	D	171.8	83.4	18.3	43.1	15.9	4.7	13.0	9.9	5.7	
	p-value of D		< 0.05	< 0.05	< 0.05	< 0.05	< 0.05	< 0.05	< 0.05	< 0.05	< 0.05
Reno	NLLH	505.4	418.4	462.5	496.0	484.4	497.6	503.1	408.8	457.4	493.2
	AIC	1016.8	846.8	932.9	1000.0	978.8	1003.2	1016.1	831.7	924.8	996.5
	D	174.0	85.9	18.8	42.0	15.6	4.7	19.1	10.1	5.5	
	p-value of D		< 0.05	< 0.05	< 0.05	< 0.05	< 0.05	< 0.05	< 0.05	< 0.05	< 0.05
# of model parameters		3	5	4	4	5	4	4	7	5	5
Model # compared to for pval			1	1	1	1	1	1	2	3	4

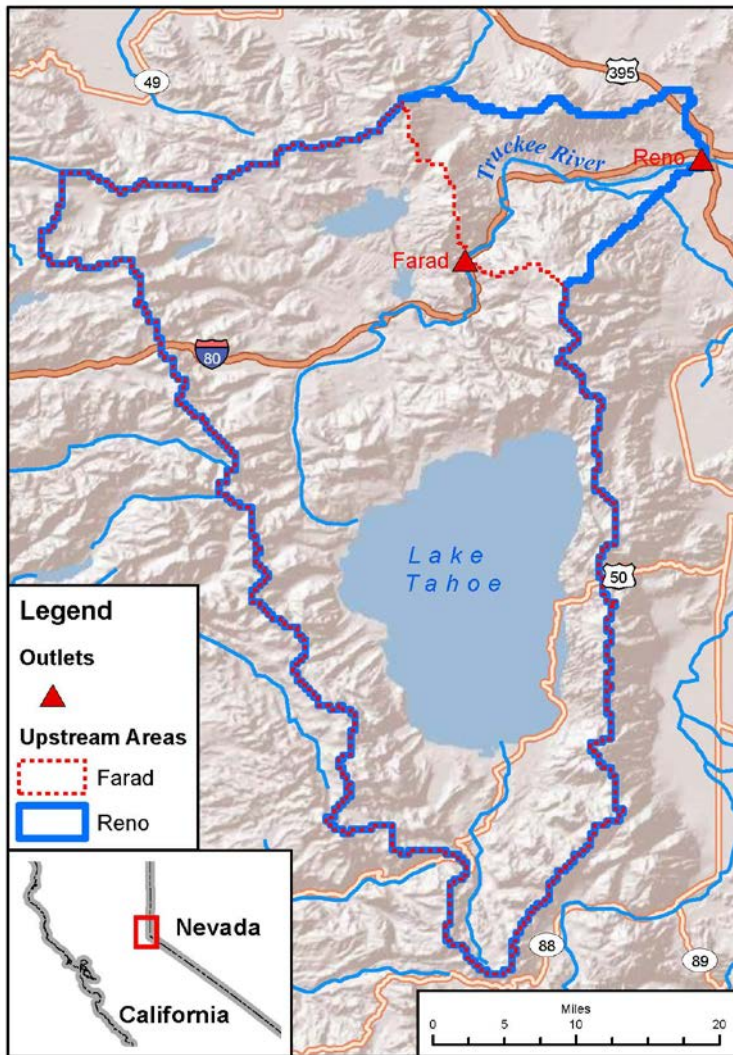
8

1  
 2 Table 3: Summary of derived model covariates for equations 2 and 3 based on historical  
 3 observations (Historical Observed) and using historical simulated data from the 234  
 4 CMIP 5 Projections (Historical Simulated Interquartile Range, IQR).

5

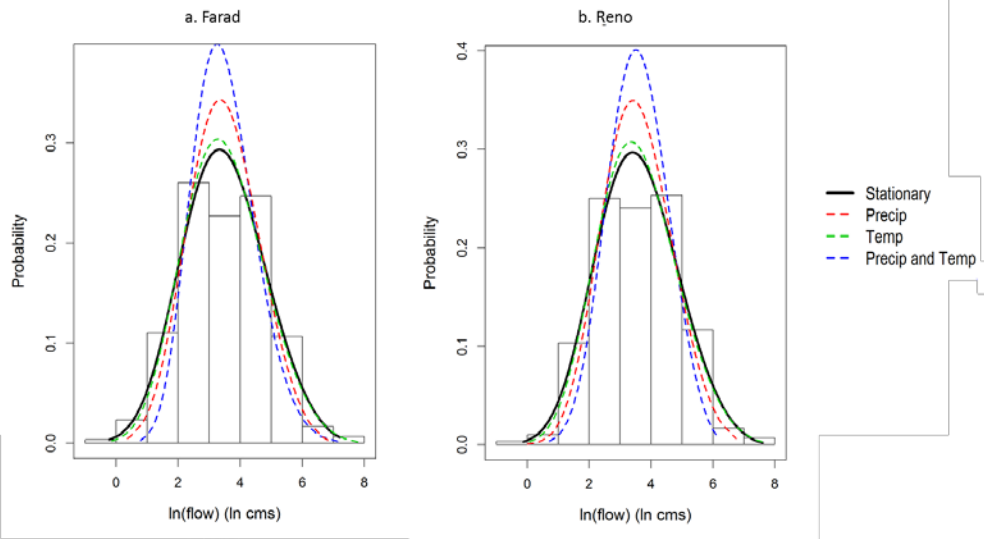
	Farad			Reno		
	Historical Observed	Historical Simulated- IQR		Historical Observed	Historical Simulated IQR	
$\beta_{0\mu}$	2.155	1.738	4.794	2.582	2.135	4.827
$\beta_{1\mu}$	0.175	0.053	0.148	0.180	0.066	0.152
$\beta_{2\mu}$	0.115	0.046	0.138	0.105	0.046	0.124
$\beta_{0\sigma}$	0.211	0.517	1.673	0.530	0.569	1.748
$\beta_{1\sigma}$	-0.013	-0.020	0.006	-0.018	-0.023	0.008
$\beta_{2\sigma}$	0.027	-0.012	0.022	0.017	-0.015	0.019
Shape ( $\xi$ )	-0.178	-0.389	-0.094	-0.275	-0.389	-0.070

6



1  
2 Figure 1: Map of model domain including the Farad and Reno gauges and their drainage  
3 areas.  
4

1



2

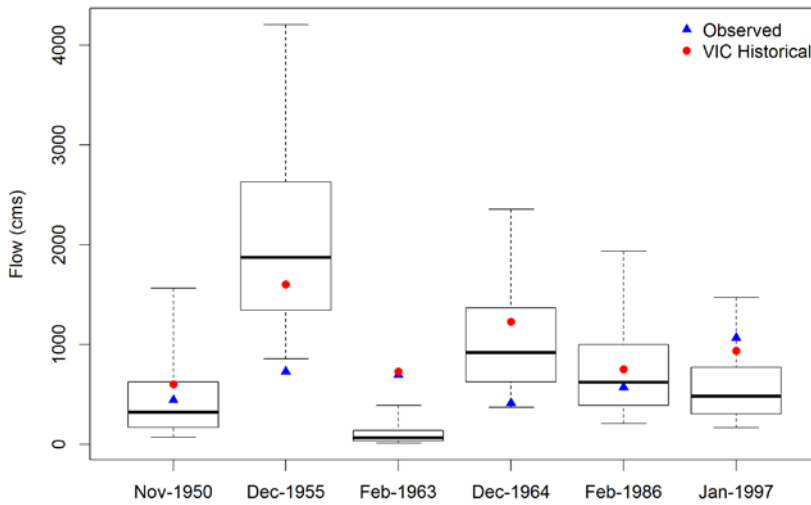
3

4

5

6

Figure 2: PDFs of fitted stationary (solid black) and non-stationary (dashed) GEV models compared to historical VIC simulated flow histogram.



7

8

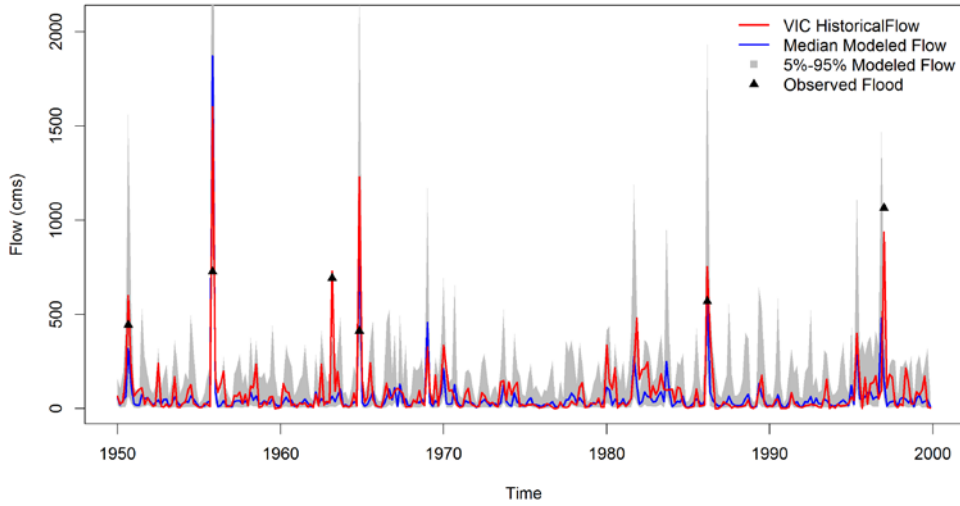
9

10

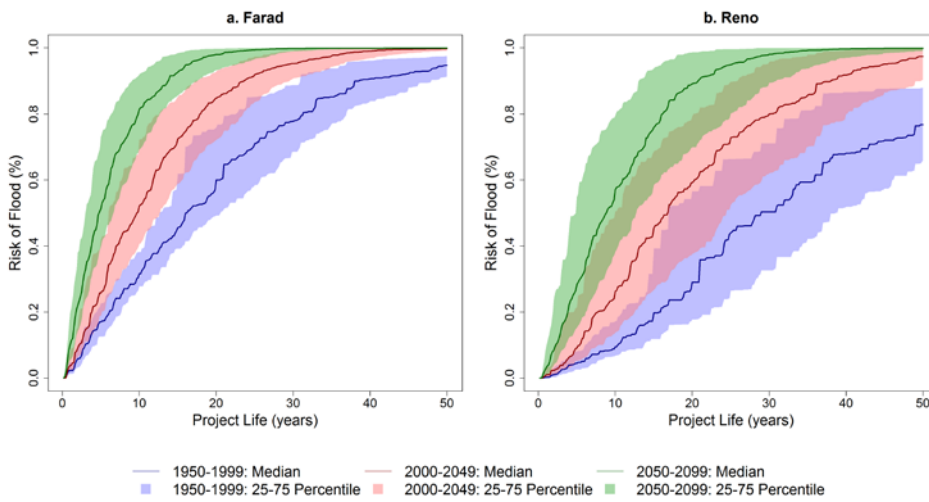
11

Figure 3: 'Observed' unregulated flow estimated from gauge records (blue triangle) compared with VIC simulated flow (red circles) and the simulated GEV distribution. Boxes span the 25<sup>th</sup> to 75<sup>th</sup> percentile of the GEV distribution for a given month and the whiskers extend to the 5<sup>th</sup> and 95<sup>th</sup> percentiles.

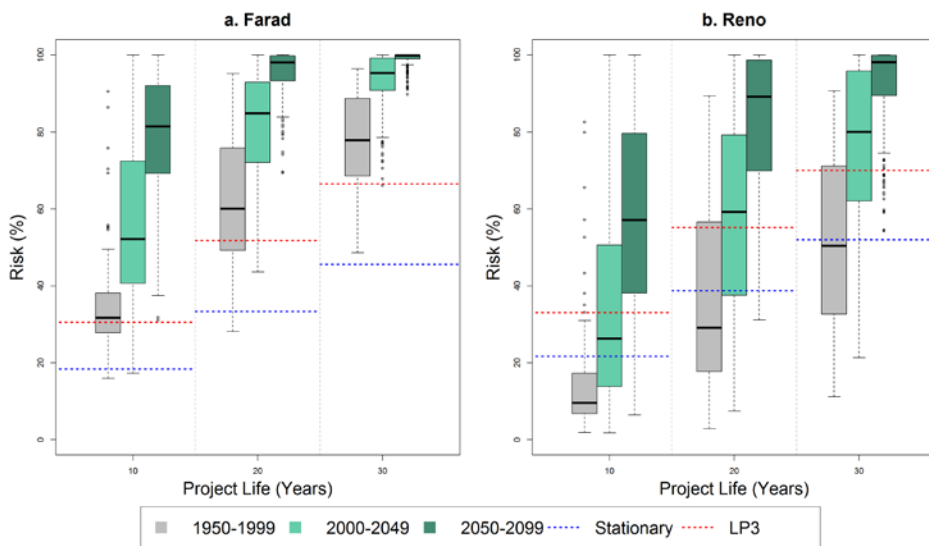
1  
2  
3



4  
5 Figure 4: VIC simulated one- day flood maximums for November through April 1950 to  
6 1999 (red lines) compared with the historical GEV distributions (blue line is median and  
7 grey shading is the 5<sup>th</sup> to 95<sup>th</sup> percentile range) and the six observed flow rates.  
8  
9

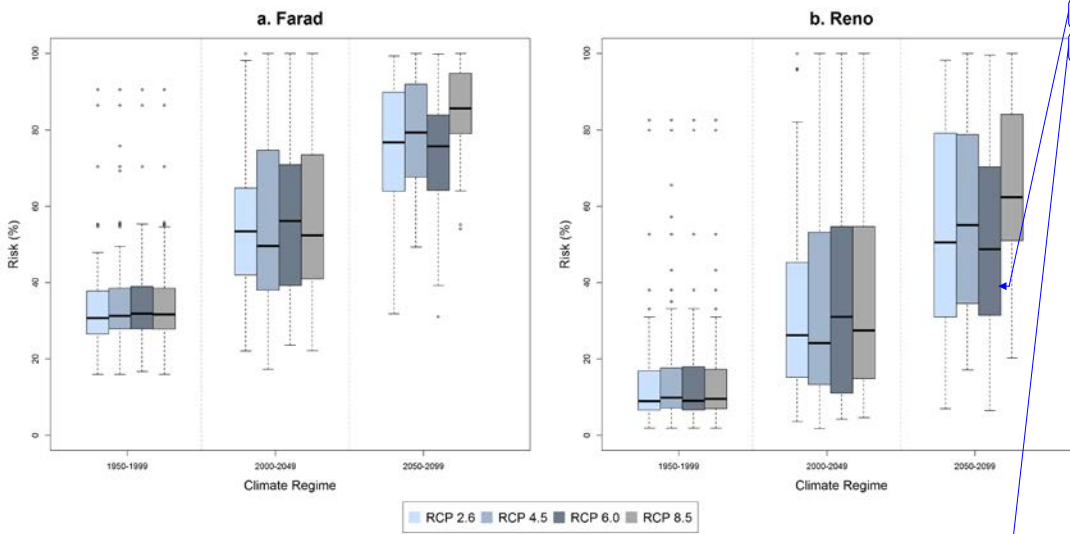


1  
 2 | Figure 5: Probability of one day flood exceeding historical maximum of [1,065cms](#)  
 3 | [37,600 cfs](#) (risk) at Farad and Reno. Solid lines represent the median risk of the 234  
 4 | climate projections and shading covers the interquartile range (i.e. 25<sup>th</sup> to 75<sup>th</sup>  
 5 | percentile).



6  
 7 | Figure 6: Boxplots of the probability of a one-day flood exceeding [1,065cms](#) [37,600 cfs](#)  
 8 | (risk) for three project life lengths (10, 20 and 30 years). Results are grouped by time  
 9 | period (1950-1999, 2000-2049 and 2050-2099). Blue dashed lines show the flood risk  
 10 | calculated from the stationary GEV model fit to the historical data.



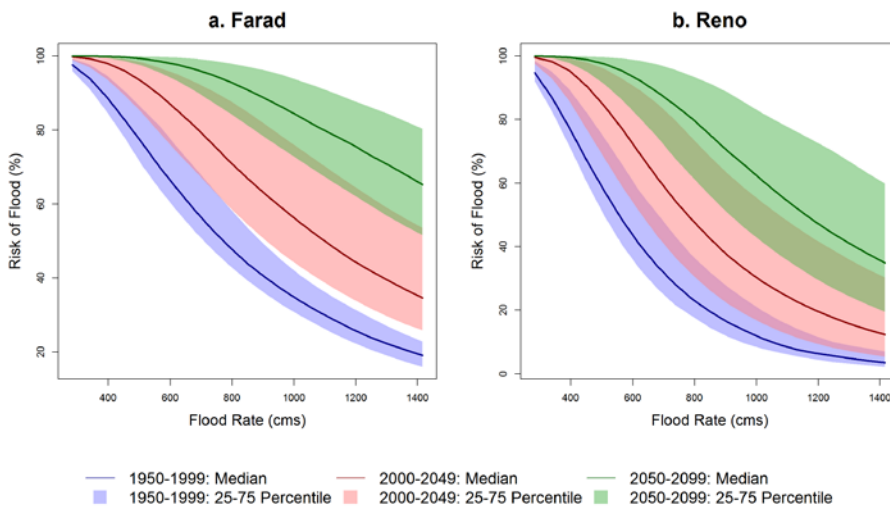


Formatted: Normal

Formatted: Font color: Black, English (U.S.)

1  
2 [Figure 7: Boxplots of the probability of a one-day flood exceeding 1.065cms \(risk\) in ten](#)  
3 [years for three fifty year periods. Results are grouped by the Representative](#)  
4 [Concentration Pathway \(RCPs\) used to drive the GCM projection. RCP 8.5 has the largest](#)  
5 [increase in greenhouse gas concentrations and RCP 2.6 the least.](#)

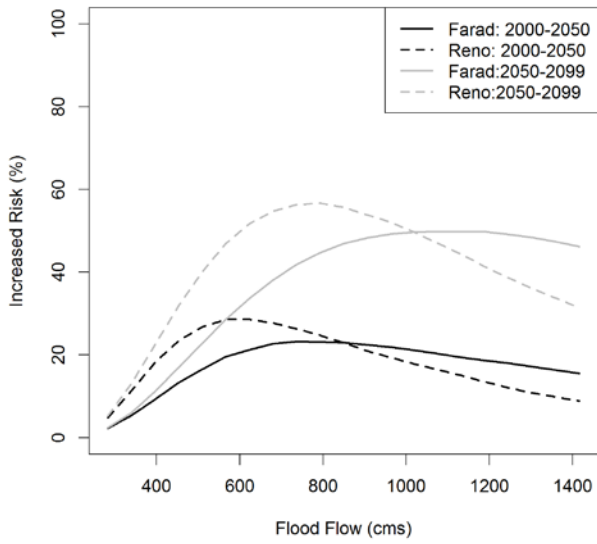
6



7

8 | [Figure 68: Probability of flood in a ten year project life \(risk\) vs. median one day flood](#)  
9 [rate \(a\) Farad and \(b\) Reno for three time periods 1950-1999 \(blue\), 2000-2049 \(red\)](#)  
10 [and 2050-2099 \(green\). Solid lines represent the median of the 234 climate projections](#)  
11 [and shading covers the interquartile range \(i.e. 25<sup>th</sup> to 75<sup>th</sup> percentile\).](#)

1



2

3 | Figure 89: Increased probability of flood occurrence for a 10 year project life (risk) from  
4 the historical period (1950-1999) to each of the two future periods 2000-2050 (black)  
5 and 2050-2099 (grey). Farad is plotted with a solid line and Reno is a dashed line.

6